

Multiple Sclerosis Lesion Analysis in Brain Magnetic Resonance Images: Techniques and Clinical Applications

Yang Ma*, Chaoyi Zhang*, Mariano Cabezas[†], Yang Song[‡], Zihao Tang*[†],
Dongnan Liu*[†], Weidong Cai*, Michael Barnett^{†§}, Chenyu Wang^{†§}

*School of Computer Science, University of Sydney, Australia

[†]Brain and Mind Centre, University of Sydney, Australia

[‡] School of Computer Science and Engineering, University of New South Wales, Australia

[§]Sydney Neuroimaging Analysis Centre, Australia

Contact e-mail: {yama5878, czha5168, ztan1463}@uni.sydney.edu.au,
yang.song1@unsw.edu.au, {mariano.cabezas, dongnan.liu, tom.cai}@sydney.edu.au,
tim@snac.com.au, michael@sydneyneurology.com.au

Abstract—Multiple sclerosis (MS) is a chronic inflammatory and degenerative disease of the central nervous system, characterized by the appearance of focal lesions in the white and gray matter that topographically correlate with an individual patient’s neurological symptoms and signs. Magnetic resonance imaging (MRI) provides detailed in-vivo structural information, permitting the quantification and categorization of MS lesions that critically inform disease management. Traditionally, MS lesions have been manually annotated on 2D MRI slices, a process that is inefficient and prone to inter-/intra-observer errors. Recently, automated statistical imaging analysis techniques have been proposed to extract and segment MS lesions based on MRI voxel intensity. However, their effectiveness is limited by the heterogeneity of both MRI data acquisition techniques and the appearance of MS lesions. By learning complex lesion representations directly from images, deep learning techniques have achieved remarkable breakthroughs in the MS lesion segmentation task. Here, we provide a comprehensive review of state-of-the-art automatic statistical and deep-learning MS segmentation methods and discuss current and future clinical applications. Further, we review technical strategies, such as domain adaptation, to enhance MS lesion segmentation in real-world clinical settings.

I. INTRODUCTION

Multiple sclerosis (MS) is a chronic inflammatory and degenerative disease of the central nervous system (CNS) with protean neurological manifestations that reflect both focal and diffuse damage to the brain and spinal cord. Visual, motor, sensory, and sphincter dysfunction are common clinical features, which in early disease usually follow a relapsing course with partial remissions; untreated, the majority of patients will develop progressive motor and cognitive disability [1]. The disease is relatively common in Caucasian populations, and both genetic and environmental factors, culminating in immune dysregulation and CNS inflammation, have been causally implicated [2]. The prevalence and incidence of MS are increasing globally, particularly in females, for unknown reasons [3]. Globally there are an estimated 2.3 million people

with MS, and after trauma, the disease constitutes the most common cause of neurological disability in young adults.

Magnetic resonance imaging (MRI) sensitively detects MS lesions and is a crucial tool for the diagnosis of MS, objective monitoring of disease progression, and the assessment of treatment efficacy [4]. In clinical trials of putative therapeutics, MRI-derived lesion metrics (number, volume, type) are critical endpoints. As such, the segmentation and quantification of MS lesions require high precision and accuracy. More recently, the advent of precision medicine has seen these metrics emerge as novel tools for informing the management of individual patients in routine clinical practice.

MS lesions are commonly annotated and measured manually by radiologists or trained neuroimaging analysts with semi-automated annotation tools in clinical trials and imaging studies. Although manual segmentation is still essential, it is impractical for broader clinical applications, since it is generally time-consuming and labor-intensive, and suffers from inter-/intra-observer biases and errors. As such, there is a growing need for fully automated tools that provide accurate and precise segmentation of MS lesions rapidly from MRI. A number of automatic segmentation methods have been proposed, and the recent incorporation of deep learning methods has rapidly accelerated the development of more accurate automatic lesion segmentation tools. However, challenges remain and current state-of-the-art techniques remain inferior to expert manual segmentation.

One of the more common problems with existing machine learning methods is poor generalization in the context of multi-center studies. Models that are trained with images from one scanner may yield poor results when tested with images from another scanner or acquired with a different protocol. Additionally, the spatial distribution and appearance of MS lesions are heterogeneous. Referenced to manually segmented ground truth data, an excellent Dice similarity coefficient (DSC) score at the group level, therefore, does not

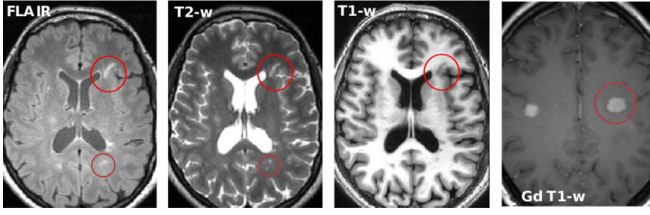


Fig. 1. T2-FLAIR, T1-w, T2-w and Gd T1-w images of brain damage. MS lesions are indicated by red circles.

guarantee a good segmentation at the individual level, which is crucial in quantitative imaging applications for clinical practice. Finally, MS lesions constitute only a small fraction of the total brain volume, resulting in a highly imbalanced dataset that poses further challenges to train models. In this survey, we provide a comprehensive review of the most recently described MS segmentation techniques, to assist imaging researchers with the development of robust, precise, and accurate lesion segmentation solutions for real-world clinical applications.

There are several previous surveys of MS lesion segmentation techniques, the majority of which were published before 2013 and focused on statistical-modeling segmentation methods [5]–[8]. Danelakis et al. [9] reviewed MS segmentation methods published between 2013 to 2018; and Kaur et al. [10] included three methods described in 2019 in addition to earlier methods. Finally, Zhang et al. [11] reviewed deep-learning methods up to 2020. However, a combined analysis of both statistical and deep-learning methods is lacking, as is a comprehensive discussion of their clinical integration and application.

In this work, we present a comprehensive survey of MS lesion segmentation methods published prior to 2021, unifying previous statistical modeling approaches with state-of-the-art deep-learning frameworks. We specifically discuss the potential for these segmentation methods to address an urgent clinical need for quantitative lesion activity analysis (the measurement of longitudinal lesion change); and also review domain adaptation solutions to lesion segmentation in multicenter, multi-scanner user scenarios [5]–[11].

II. IMAGING THE MS LESION

A. Common MRI Modalities

To visualize MS lesions, four imaging sequences are commonly acquired: PD-weighted (PD-w), T1-weighted (T1-w), T2-weighted (T2-w), and T2 fluid-attenuated inversion recovery (T2-FLAIR) imaging [12], as shown in Fig. 1. Generally, structural T1-w and FLAIR are most frequently used in clinics and contain all necessary information to identify MS lesions with modern 1.5 and 3.0T scanners, while PD-w and T2-w images offer superior visualization of lesions in the posterior fossa.

Compared with normal white matter, MS lesions appear hypointense on T1-w images; and are usually hyperintense on T2-w, PD-w, and FLAIR images (Fig. 1). The identification of lesions on PD-/T2-w imaging is hampered by the similarity

of cerebrospinal fluid (CSF) and lesional voxel intensities, particularly in the commonly involved peri-ventricular white matter zone. T2-FLAIR imaging, which attenuates CSF signal, permits hyperintense MS lesions to be seen to a better advantage. Therefore, a multimodal approach provides the best opportunity to robustly and accurately segment MS lesions.

B. MS Lesion Subtypes

MS lesions are heterogeneous both in morphology and signal characteristics. Most commonly, MS lesions appear as small ovoid hyperintensities on T2-w, PD-w, and FLAIR images; and are hypointense on T1-w images. Lesion appearance may evolve serial imaging, due to changes in lesion water content, myelin and axon density, inflammatory cell populations, and gliosis. Rarely, highly inflammatory lesions may liquify, developing a central necrotic zone with similar voxel intensities to CSF. As a consequence, they may appear hypointense on FLAIR-imaging and be missed by models primarily trained with hyperintense lesion masks. Necrotic lesions in the periventricular lesions may be absorbed into the CSF, rendering them undetectable by both conventional and model-derived image analyses.

According to the current revision of diagnostic criteria for MS patients [4], dissemination of lesion in time (DIT) and space (DIS) are essential for the diagnosis of MS.

DIT can be inferred from a single scan by the simultaneous presence of T2-w/PD-w hyperintense lesions that exhibit gadolinium contrast-enhancement on T1-w imaging, indicative of recent inflammatory activity and associated breakdown of the blood-brain barrier, and non-enhancing lesions. DIT can also be determined by the presence of new MS lesions on a subsequent (follow-up) MRI scan.

DIS is assessed by detecting at least two of the four MS-typical lesion subtypes (juxtacortical, cortical, periventricular or infratentorial, or spinal cord) in a single scan:

- *Juxtacortical lesions* are usually small, ellipsoid, or linear in appearance, and located adjacent to the cerebral cortex. However, their small size hinders detection, especially when images are acquired with a slice thickness greater than the lesion size (due to partial volume). High resolution gapless 3D FLAIR images, routinely acquired in many larger MS centers, partially alleviate this issue.
- *Cortical lesions* occur within the cortex; while commonly identified in histopathological MS tissue, they are rarely detected in-vivo with conventional clinical scanning protocols. Non-conventional techniques such as double inversion recovery imaging, which suppresses both CSF and normal white matter signal, may improve cortical lesion detection and segmentation [13]. Additionally, MP2RAGE, a novel T1-w sequence, is reported to be highly sensitive for cortical lesions [14].
- *Periventricular lesions* are usually 5-10 mm corona-like structures that involve the white matter adjacent to the ventricular CSF. While relatively easy to detect with FLAIR imaging, their heterogeneous shape and intensity make the delineation of their contours a difficult task.

- *Infratentorial lesions*, which involve the brainstem or cerebellum lesions, are usually small and may be difficult to discern on FLAIR imaging. Visualized to better advantage with T2-w imaging, infratentorial lesions are frequently symptomatic and may portend a worse prognosis. Accurate segmentation and quantitation may therefore constitute an important and clinically relevant biomarker. A discussion of spinal cord lesions is outside the scope of this review.

In previous reviews, discussion of lesion identification techniques for different lesion subtypes was limited, and primarily focused on the segmentation of white matter hyper-intensities (regardless of their subtype); or cortical lesions.

III. LESION SEGMENTATION FRAMEWORK

Several challenges arise when developing segmentation models for MRI data acquired from clinical sites due to intensity inhomogeneity [15], [16] and imaging noise [17], [18] inherent to the scanner acquisition. Pre-processing steps are commonly applied to minimize this impact prior to the implementation of the lesion segmentation algorithm. Common pre-processing steps and their 3D representation are demonstrated in Fig. 2 and summarised as follows:

- *Co-registration* aligns different MRI sequences to the same 3D space in order to benefit from multi-contrast information for lesion segmentation. Most methods perform rigid transformations followed by image resampling with interpolation [19], [20].
- *Denoising* reduces the noise introduced by the acquisition phase, improving the signal-to-noise-ratio. A wide range of methods, adopted from general computer vision, are used and include the non-local means algorithm [17], anisotropic diffusion filter [15], and (3D) Gaussian low-pass filter [16], [21].
- *Bias Correction* ameliorates the intensity inhomogeneities of a given image. Due to imperfections in the acquisition magnet, voxels of the same tissue can have different intensities in different brain regions. Inhomogeneity correction is most commonly performed with the N3 normalisation technique [15], [16] and its improvement, the N4 normalisation technique [17], [18], [22]–[24].
- *Skull stripping* is used to remove the skull along with other non-brain tissues that may influence the segmentation performance. Two common strategies are template-based and edge-based approaches. Existing toolboxes include VolBrain [17], [18], bet2 [16], and ROBEX [25].

Following image pre-processing steps, both supervised and unsupervised machine learning techniques have been applied to the task of lesion segmentation. The principal difference between these broad categories relates to whether labeled data is used for training. Unsupervised techniques generally aim to simulate the intuitive processes that permit humans with expert domain knowledge, in this case, clinicians and neuroscientists, to accurately segment lesions; and do not rely on annotated data for model training. Using training data labeled by human

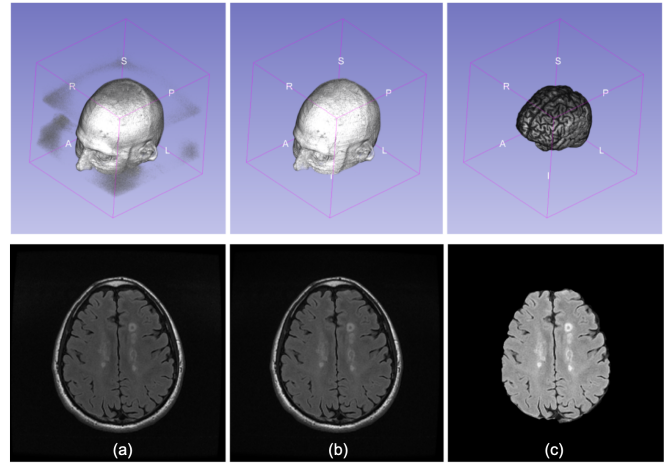


Fig. 2. 3D visualisation of pre-processing steps. (a) Original MRI input. (b) Normalisation with N3 bias correction. (c) Skull stripping.

experts, supervised methods learn the representation of MS lesions using a training process. Training these techniques normally involves explicit feature engineering or the use of deep neural networks. Furthermore, the format of the input data includes 2D-image input (pixel-level) and 3D-volume input (voxel-level).

Supervised methodologies are differentiated into statistical and deep-learning methods:

- *Statistical methods* usually apply statistical models to perform probabilistic segmentation on the original data or the hand-crafted features. The engineered features normally incorporate useful interpretation for the MS lesions from the initial input data.
- *Deep-learning based methods* use deep convolution neural networks (CNNs) as voxel classification models for segmenting MS lesions. Borrowing from the architecture of CNNs widely used for computer vision tasks on general images, these methods can learn more comprehensive information and achieve greater performance than statistical models.

Following these definitions, the state-of-the-art of MS lesion segmentation techniques are reviewed in the following sections and summarized in Table I.

A. Statistical Lesion Segmentation Methods

1) *Unsupervised methods*: Early MS lesion segmentation approaches were reliant upon unsupervised methods, which do not rely on manually annotated training data, but rather identify and segment lesions based solely on the voxel-wise intensity information of the input brain MRI. In the majority of described methods, whole brain tissue is segmented before the identification of MS lesions with a number of different techniques. In general, the Expectation Maximization (EM) algorithm [15], [17], [33], and Gaussian Mixture Modelling (GMM) [21], [22], [29] are frequently applied to classify each voxel into CSF, WM and GM clusters, and lesions are secondarily identified as outliers. In contrast, other authors

TABLE I
REVIEW OF MS SEGMENTATION METHODS

Method	Supervision	Strategy	Data Handling	MRI Data	Classifier
Weiss et al., 2013 [26]	Unsupervised	Statistical	2D input	T1-w, T2-w	Dictionary based
Knight et al, 2016 [21]	Unsupervised	Statistical	2D input	T2-FLAIR	Edge-based model
Roy et al, 2017 [27]	Unsupervised	Statistical	2D input	T1-w, T2-w, PD-w	Background generation and binarization
Hill et al, 2015 [28]	Unsupervised	Statistical	2D input	T1-w, T2-w, PD-w	IJM
Tomas-Fernandez et al, 2015 [29]	Unsupervised	Statistical	3D input	T1-w, T2-w, T2-FLAIR	MOPS
Tomas-Fernandez et al, 2016 [30]	Unsupervised	Statistical	3D input	T1-w, T1-w Gd, T2-w, T2-FLAIR	GMM
Urien et al, 2016 [31]	Unsupervised	Statistical	3D input	T1-w, T1-w Gd, T2-w, T2-FLAIR, PD-w	Max-tree
Koley et al, 2016 [32]	Unsupervised	Statistical	3D input	T2-w, T2-FLAIR	3D Gaussian template
Catanese et al, 2015 [33]	Unsupervised	Statistical	3D input	T1-w, T2-w, T2-FLAIR	EM
Beaumont et al., 2016 [17], [34]	Unsupervised	Statistical	3D input	T1-w, T1-w Gd, T2-w, T2-FLAIR, PD-w	EM
Roura et al., 2016 [15]	Unsupervised	Statistical	3D input	T1-w, T2-FLAIR	Anisotropic diffusion
Doyle et al., 2016 [22]	Unsupervised	Statistical	3D input	T1-w, T1-w Gd, T2-FLAIR	GMM
Santos et al., 2016 [16]	Supervised	Statistical	2D input	T1-w, T1-w Gd, T2-w, T2-FLAIR, PD-w	MLP
Andermatt et al, 2017 [35]	Supervised	Deep-learning	2D input	T1-w, T2-w, T2-FLAIR, PD-w	RNN
Havaei et al, 2016 [36]	Supervised	Deep-learning	2D input	T1-w, T2-w, T2-FLAIR	CNN
Zhang et al., 2018 [37]	Supervised	Deep-learning	2D input	T1-w, T2-FLAIR	CNN
Ackaouy et al., 2020 [38]	Supervised	Deep-learning	2D input	T1-w, T2-w, T2-FLAIR	Seg-JDOT
Steenwijk et al., 2013 [39]	Supervised	Statistical	3D input	T1-w	k-NN
Geremia et al., 2013 [40]	Supervised	Statistical	3D input	T1-w, T2-w, T2-FLAIR	RF
Maier et al., 2015 [41]	Supervised	Statistical	3D input	T1-w, T2-w, T2-FLAIR, PD-w	RF
Jog et al., 2015 [23]	Supervised	Statistical	3D input	T1-w, T2-w, T2-FLAIR	Decision Trees
Mahbod et al., 2016 [42]	Supervised	Statistical	3D input	T1-w, T1-w Gd, T2-w, T2-FLAIR, PD-w	ANN
Doyle et al., 2017 [43]	Supervised	Statistical	3D input	T1-w, T1-w Gd, T2-FLAIR	IMaGe
Ghafoorian et al., 2015 [44]	Supervised	Deep-learning	3D input	T1-w, T2-w, T2-FLAIR, PD-w	CNN
Vaidya et al., 2015 [45]	Supervised	Deep-learning	3D input	T1-w, T2-w, T2-FLAIR, PD-w	CNN
McKinley et al., 2016 [46]	Supervised	Deep-learning	3D input	T2-FLAIR	CNN
Brosch et al., 2016 [47]	Supervised	Deep-learning	3D input	T1-w, T2-w, T2-FLAIR	CNN
Valverde et al., 2016 [18]	Supervised	Deep-learning	3D input	T1-w, T1-w Gd, T2-w, T2-FLAIR, PD-w	CNN
Valverde et al., 2017 [48]	Supervised	Deep-learning	3D input	T1-w, T2-w, T2-FLAIR	CNN
Roy et al., 2018 [24]	Supervised	Deep-learning	3D input	T1-w, T2-w, T2-FLAIR, PD-w	CNN
Isensee et al., 2018 [49]	Supervised	Deep-learning	3D input	T1-w, T1-w Gd, T2-FLAIR	CNN
Nair et al., 2019 [50]	Supervised	Deep-learning	3D input	T1-w, T1-w Gd, T2-FLAIR	CNN

have described unsupervised methods, such as the max-tree algorithm, which estimate lesions directly and obviate the need for tissue clustering [31].

Specifically, in the method proposed by Roura et al. [15], brain tissue types were delineated using Statistical Parametric Mapping (SPM) and lesions then segmented by applying an intensity threshold on the FLAIR image. In Doyle et al. [22], brain tissues were firstly clustered using a weighted Gaussian tissue model, and the left-over outlier voxels considered as MS lesion candidates. In a similar technique described by Catanese et al. [33], the EM algorithm was applied to cluster candidate voxels into CSF, WM, and GM. Next, a graph-cut technique was applied to detect the lesions as outliers of the segmented tissues. In 2016, Knight et al. [21] combined fuzzy clustering with an edge-based model on the original input. Thresholding and a false-positive reduction method were then applied to obtain the final lesion segmentation prediction.

2) *Supervised methods*: Supervised lesion segmentation methods aim to extract engineered features from the input images for training statistical models with annotated data. Common features include spatial and intensity information.

For example, features can be defined as non-local relationships and symmetry [40]. Various statistical learning models are applied to generate the segmentation, including the k-nearest neighbor (kNN) classifier [39], a random forest (RF) classifier [40], [41], decision trees [23]), a multi-layer perceptron (MLP) classifier [16], [42], or a Markov random fields (MRF) [43] approach.

For example, Steenwijk et al. [39] proposed to use a set of probabilistic atlases as priors for GM, WM, and CSF tissues, called tissue type priors (TTPs). These TTPs are then combined with other extracted features to create a feature vector, and then train a kNN classifier to predict whether a voxel belongs to a lesion or not. Geremia et al. [40] engineered symmetry, space, and intensity features and trained an RF classifier. Similarly, Maier et al. [41] generated spatial features by pre-processing the input voxels via intensity normalization prior to the RF classifier training, followed by post-processing techniques based on the intensity and morphology information of the initial prediction. Another approach using multi-output decision trees and spatial and intensity features was presented by Jog et al. [23]. In Mahbod et al. [42], engineered

features based on the intensity and spatial information were fed to an artificial neural network (ANN) to provide the final segmentation output. Similarly, Santos et al. [16] proposed to use a simple MLP classifier with one hidden layer to obtain MS lesion segmentation. In Doyle et al., segmentation was handled with an Iterative Multilevel Probabilistic Graphical model (IMaGe) with two MRF blocks at the region level [43] based on tissue class priors and local and neighboring information.

B. Deep-learning based Lesion Segmentation Methods

Compared to classical statistical methods, deep-learning methods can generate representative features automatically during training using specific layers such as convolutional blocks. By processing a complex representation in a high-dimensional feature space, these methods can achieve better performance. Typically, deep-learning based lesion segmentation methods employ encoder-decoder CNN architectures, such as the U-Net [51], [52].

One of the first deep learning approaches to segment MS lesions was presented by Ghafoorian et al. with a five-layer CNN network [44]. At that point in time, CNN architectures were mostly used for image classification. Ghafoorian's method essentially used this approach to obtain a voxel-level segmentation by classifying a patch for each possible image voxel. In the same year, another 3D network was developed by Vaidya et al. with four layers for multi-channel 3D patches [45]. Similarly, Valverde et al. also extended this approach to 3D patches to include 3D information from the processed MRI data to predict the label of the center voxel [18], [48]. The authors also proposed a cascaded architecture to provide high sensitivity in the first network, with the trade-off of an increased number of false positives; and a second network to counter the effect of false positives.

Another interesting 2D approach was presented by Havaei et al. [36]. In their segmentation methodology, multi-channel 2D images were fed as input into a multi-stage convolutional pathway to deal with subjects that had different numbers and types of input images. The proposed network contains a front-end block, an abstraction block, and a back-end block. The front-end block uses independent convolutional blocks to yield information mapping of different modalities, and the total number of input modalities is flexible per case. The abstraction layer then interprets the statistical information of the input mapping; finally, the front-end block, with two convolutional layers, generates a pixel-wise probability classification output. In order to benefit from multichannel information, Roy et al. developed a CNN structure with multiple convolutional pathways for 2D patches of two independent input modalities (FLAIR, T1-w imaging) [24]. The output of these two pathways is concatenated and a final convolutional pathway used to yield the lesion segmentation.

More recent studies have favored encoder-decoder architectures to reduce network complexity while maintaining a similar performance, or in some instances, better performance. Brosch et al. [47] developed a deep 3D convolutional seven-

layer encoder network with shortcut connections (CENs). The authors defined a mapping function to transfer multi-channel MRI to probabilistic lesion masks. High-level representations of the input were abstracted using convolutional layers, along with pooling layers to reduce the spatial size of the representation and the number of parameters for training.

In related work, McKinley et al. proposed 'Nabla-net', a deep CNN for MS lesion segmentation [46] that also adopted an encoder-decoder structure to extract higher-level representations of the input data with 18 layers in total. The authors subsequently described 'DeepSCAN' [53], another architecture that uses 3D input patches and converts them into 2D slices on the encoding path. Then, rather than recovering the initial 3D shape, segmentation is performed on 2D slices to obtain the final output. The method involves an uncertainty-based loss function using a combination of focal loss and label-flip loss to account for noisy labels. Finally, the same group extended their approach to simultaneously segment brain structures and lesions [54].

Another example of an encoder-decoder architecture for MS lesion segmentation and uncertainty prediction was described by Nair et al. [50]. Their work explored four voxel-based uncertainty estimate measures using the Monte Carlo (MC) dropout technique presented by Gal and Ghahramani [55]. Gal and Ghahramani showed that minimization of the Kullback-Leibler (KL) divergence, which captures the uncertainty in the model, is equivalent to the minimization of cross-entropy loss of a network with dropout applied. The uncertainty measures explored by Nair et al. included the predicted variance learned from the training data and three stochastic sampling-based measures including predictive entropy, the variance of the MC samples, and mutual information. Using these uncertainty measures, they also improved voxel-wise true positive and false-positive rates, which can benefit the identification of small lesions.

Rather than using normal convolutions to represent local relationships between pixels, Andermatt et al. implemented an architecture based on multidimensional gated recurrent units (MD-GRU) [35]. A gated recurrent unit (GRU) [56] is a feature extraction module based on convolution and a gating mechanism, working as a building block for recurrent neural networks (RNN). These GRU layers are capable of encoding neighbourhood relationships without the constraint of the traditional convolution kernel size. The authors also reported that this modification allowed the model to converge faster.

Finally, based on the U-Net architecture, Isensee et al. described the nnU-Net segmentation framework for general medical image segmentation [57]. This framework dynamically adapts itself to the specifics of any given training dataset. The essence of this approach is the in-depth design of adaptive preprocessing, training schemes, and inference. All design choices required to adapt to new segmentation tasks are made in a fully automated manner, avoiding the need for manual interaction. For each task, n-fold cross-validations are systematically performed for different U-Net models; and

the mean foreground Dice score employed as the criterion to choose and submit a final model. This framework was tested on the MS lesion segmentation task, outperforming the 3D-to-2D (DeepSCAN) CNN architecture.

IV. CLINICAL LESION SEGMENTATION APPLICATIONS

In Section III, we provided a detailed survey of the reviewed cross-sectional lesion segmentation methods. In practical clinical applications, analysis of longitudinal lesion evolution is an important measure of disease progression and treatment efficacy that informs optimal management of individual patients. Additionally, the clinical adoption of fully automated segmentation methods is hampered by domain bias imparted by different MRI acquisition protocols, in which a specific model may underperform due to inter-scanner/protocol variances between the training and testing dataset. In this section, we will further discuss technical approaches to address these key translational requirements.

A. Lesion Activity Analysis

To assess the lesion evolution over time, longitudinal analysis of a series of MRI images is required. Methods that process each time point independently are less reliable due to differences in the images that can cause discrepant segmentation masks when temporal information and redundant features (such as stable image regions) are not considered. Most methods apply subtraction as a simple technique to remove “stable” disease and highlight temporal changes. Some unsupervised strategies apply thresholding to these subtraction images to classify new lesions, such as the works of Ganiler et al. [58] and Cabezas et al. [59].

Jain et al. presented a subtraction-based framework called MSmetrix-long, using the lesion segmentation from two time points and subtraction imaging [60]. Their framework firstly applied MSmetrix-cross [61] to get a cross-sectional lesion segmentation of each time point separately. Then the FLAIR-based subtraction images were created for the two directions via co-registration and bias normalization. Similarly, Schmidt et al. [62] presented an approach to detect lesion changes using cross-sectional masks of each timepoint [63] and their FLAIR intensity differences. Using the intensity differences in the normal appearing white matter region, they defined a rule to detect significant intensity differences for the lesion areas.

Using statistical modeling, Cerri et al. [64] proposed a methodology capable of segmenting multiple time points at the same time. Extending their cross-sectional approach [65] where each input image is processed separately, they exploited the common spatial features shared by all the time points from the same subject. Subject-specific latent variables were introduced to the segmentation priors and likelihood, linking different time points with a statistical dependency.

The first CNN architecture for new T2-w lesion segmentation in longitudinal brain MR images was proposed by Salem et al. [66]. By using an unsupervised registration module to obtain the deformation field between timepoints with a supervised module for lesion segmentation, the overall method

can be trained in an end-to-end fashion. In the same year, Gessert et al. [67] applied a CNN model for lesion activity segmentation using an attention mechanism [68]. Specifically, the authors engineered an architecture with an independent encoding pathway for each timepoint. Then the pathways are fused with the bottleneck of the network and the last few layers of the CNN concatenated to the fusion features to generate the final segmentation. As an extension of this work, Gessert et al. described another fully 4D architecture to segment lesions over multiple time points [69], proposing a 3D ResNet-based multi-encoder-decoder CNN architecture in which, assuming the number of time points is T , a T -path encoder with shared weights is used to process all the input time points in parallel. Temporal aggregation is then completed via convolutional gated recurrent units (convGRUs), which are also employed as long-range connections from the encoders to decoders.

B. Domain Adaptation

The intensity contrast of brain tissues and MS lesions varies from the scanner to scanner, and even within the same scanner depending on the choice of acquisition parameters. Therefore, MS lesion segmentation methods in clinical practice can face several issues when using images from different domains due to the so-called domain shift issue. Multi-source domain adaptation and harmonization techniques aim to adapt a model to data acquired from different sources. This process can be achieved in a supervised manner when labels of the new domain are available; or in a completely unsupervised manner, when only the source of the new domain is known.

Ghafoorian et al. [70] studied the effectiveness of fine-tuning on a fitted model with additional annotated data from a new target domain. Experiments were conducted on a CNN, where the parameters of the shallowest i th layers were frozen and the remaining $d - i$ layers were fine-tuned with dataset D from another domain. In addition, the optimal number of frozen layers and the smallest size of the fine-tuning dataset D for a proper adaptation were also investigated.

Based on the assumption that FC layers are more sensitive to domain bias than CNN layers, Valverde et al. [71] proposed a few-shot supervised technique by re-training the FC layers of the source model with target images to tackle domain adaptation. In general, encoded knowledge in the source model can be effectively adapted to an unseen target intensity domain. This is because convolutional layers contain related features that can be transferred to unseen data while only re-training the FC layers. In that sense, domain adaptation is performed by retraining all or some of the source FC layers using images from the target domain. Re-use of implicit knowledge trained on the source model significantly lowers the number of weights required to optimize on the target model, reducing the requisite number of training images and avoiding over-fitting of the model.

For supervised domain adaptation, sub-structure re-training is another effective approach in addition to the adversarial learning strategy, given access to the labels for both source and target domains. In contrast, generative adversarial networks

(GAN) have been applied to alleviate problems that arise in the context of limited amounts of training data in unsupervised settings. Zhang et al. presented MS-GAN, an MS lesion segmentation tool [37] in which a generator network (G), based on the multi-channel encoder-decoder structure, is combined with multiple discriminator networks (D) for different input channels. By taking advantage of adversarial training, the authors achieved precision lesion segmentation without the need for experimental parameter tuning or other pre- or post-processing steps.

Kamnitsas et al. investigated unsupervised domain adaptation using adversarial neural networks to counter the effects of domain shift [72]. For the test domain, this method does not require additional annotation, and the generator is a fully convolutional neural network (FCN) for the segmentation task. A domain discriminator is implemented as a second neural network that distinguishes between images from the source and target domains. The training of the discriminator is exposed to the generator and vice versa. In that manner, the generator tries to increase the domain classification loss, thus helping to extract fewer domain-specific features and making the segmentation less sensitive to domain change.

Similarly, Palladino et al. [73] explored cycle-consistent adversarial networks (CycleGAN) to map the distribution of the source domain to the target domain and a 3D U-Net trained in the target domain to segment the style-transferred images. CycleGAN [74] is a type of GAN architecture proposed for style-transfer commonly used with unpaired data (i.e. images from the same subject in different domains). The generator is designed to find a mapping function that makes the source domain-derived images indistinguishable from real target images. Furthermore, the network has an inverse mapping, creating a cycle consistency loss for the entire framework. Both generator and discriminator follow CNN-based encoder-decoder architectures.

In addition, Ackaouy et al. [38] proposed a medical image segmentation framework called Seg-JDOT that uses unsupervised optimal transport for domain adaption. This framework ensures similar inference results for a model within different domains sharing similar representations. Tested on MS segmentation task with a 3D U-Net architecture, the model yielded promising performance in the target domain over standard training.

Finally, Dewey et al. [75] explored a different path by directly harmonizing the contrast of the input images among different domains with an architecture called DeepHarmony. The model is based on the U-Net architecture with additional concatenation steps between input contrasts and the final feature map, only altering the input contrasts and not creating entirely new contrasts. The test set included a small overlap cohort ($n = 8$) from two different acquisition protocols. The evaluation on this set showed a reduced inconsistency between the generated images with different inputs.

V. EVALUATIONS

The evaluation and comparison of different models proved difficult since not all of the reviewed methods made their datasets and trained models publicly available for evaluation. In this survey, we have grouped the methods that used a common public dataset for evaluation.

A. Public Datasets

Table II summarizes the most common public databases used by the methods discussed in this paper. The methods not listed in Table II used proprietary databases for their research.

The ISBI 2015 challenge focused on longitudinal lesion segmentation task [76]. All scans were acquired using the same protocol on a 3.0 Tesla MRI scanner. Training data provided by this challenge was derived from 5 subjects with a consecutively acquired brain MRI scans (mean of 4.4 time-points). The challenge also provided another two test sets from 10 and 4 subjects, respectively. Consecutive timepoints were acquired with a one-year gap. All images were annotated by two human experts, yielding a consensus delineation. This challenge additionally provided preprocessed images, following bias correction using N4 algorithm, skull and dura stripping, and rigid registration to 1mm isotropic MNI template.

The MICCAI 2016 challenge was held in 2016, providing a high-quality database of 53 MS cases acquired using different scanners following the same Observatoire français de la sclérose en plaques (OFSEP) protocol recommendations [77]. For each MS patient scan, seven expert manual annotations were gathered, and a consensus ground truth was provided. The challenge organizers provided raw images and preprocessed images. The preprocessing steps included denoising with a non-local means algorithm, rigid registration of each modality to the FLAIR image, skull-stripping using volBrain based on T1 image, and bias correction using the N4 algorithm.

B. Evaluation Metrics

Common performance evaluation metrics such as accuracy and F1 score, are listed in Table III.

For the ISBI 2015 challenge, a set of different metrics were also evaluated. Similar to MICCAI 2016, this challenge also applied Dice overlap and average symmetric surface distance for evaluating the ability to delineate each lesion. The challenge also used voxel-wise metrics including positive predictive value (PPV), true positive rate (TPR), absolute volume difference (AVD), and lesion-wise metrics including the lesion true positive rate (LTPR), and the lesion false positive rate (LFPR).

Similarly, for the MICCAI 2016 challenge, the average surface distance and Dice overlaps were used as the primary metrics for algorithm evaluation. The precision of the contour delineation was emphasized due to its importance for calculating the total volume of lesions, a crucial determinant of disease burden. The challenge also used the F1 score to evaluate the detection rate of the algorithms, recognizing the importance of lesion count as a criterion for MS diagnosis [4],

TABLE II
PUBLIC DATABASES USED BY DISCUSSED METHODOLOGIES

Database	MRI modalities	Scanners	Methodologies
MICCAI 2008	T1-w T2-w T2-FLAIR	3T SIEMENS	Geremia et al., 2013 [40] Havaei et al, 2016 [36] Brosch et al., 2016 [47] Valverde et al., 2017 [48]
ISBI 2015	T1-w T2-w T2-FLAIR PD-w	3T PHILIPS	Ghafoorian et al., 2015 [44] Tomas et al, 2015 [29] Maier et al., 2015 [41] Catanese et al, 2015 [33] Jog et al., 2015 [23] Vaidya et al, 2015 [45] Roy et al., 2018 [24]
MICCAI 2016	T1-w T2-w T2-FLAIR PD-w T1-w Gd	3T GE 3T SIEMENS 1.5T-SIEMENS 3T PHILIPS	Roura et al., 2016 [15] Knight et al, 2016 [21] Doyle et al., 2016 [22] Urien et al, 2016 [31] Beaumont et al., 2016 [17] McKinley et al., 2016 [46] Valerde et al., 2016 [18] Mahbod et al., 2016 [42] Santos et al., 2016 [16] Tomas et al, 2016 [30]

and, more critically, as an objective measure of disease activity that facilitates the monitoring of treatment efficacy.

In summary, the Dice coefficient for segmentation and the correct detection ratio (or true positive fraction in terms of detection) for lesion detection is the most commonly employed metrics.

C. Comparisons of Reviewed Methods

For the ISBI 2015 challenge, the evaluation of the five participating methods reviewed here is summarized in Fig. 5. CNN-based architectures with 3D inputs, such as the work of Vaidya et al. [45], outperformed other methods in terms of the ability to detect lesions. Similarly, a comparison of the reviewed methods that participated in the MICCAI 2016 challenge is summarized in Fig. 3. There were clear variations in performance while testing across data from different centers. Fig. 4 shows the compound performance in terms of the average Dice and F1 score of these methods. In general, supervised methods with 3D inputs, such as described by McKinley et al. [46] and Valverde et al. [18], outperformed other strategies. In contrast, unsupervised methods and methods using 2D image sequences seemed to have a lower performance [9].

In terms of supervised classification, the performance was more robust when a deep learning model or random forest was applied. Deep learning currently dominates the field, with the majority of recent works on lesion segmentation focusing on CNN-based models, and specifically U-Net architectures. Deep learning methods have been applied to both the lesion activity segmentation task and the multi-source domain adaptation task with promising results that approximate the performance of the average human expert rater.

However, the performance and accuracy of a particular

TABLE III
EVALUATION METRICS COMMONLY USED FOR MS SEGMENTATION

Metric Name	Equation
Accuracy	$\frac{TP+TN}{TP+TN+FP+FN}$
Sensitivity (Correct detection ratio)	$\frac{TP}{TP+FN}$ $\left(\frac{TP}{MS}\right)$
Specificity	$\frac{TN}{TN+FP}$
Dice similarity coefficient (Kappa Index)	$\frac{2TP}{2TP+FN+FP}$ $\left(\frac{2TP}{AS+MS}\right)$
Error rate	$\frac{FP+FN}{TN+TP+FN+FP}$
Fallout	$\frac{FP}{TP+TN}$
Extra fraction	$\frac{FP}{TP+FN}$
Overlap objects fraction	$\frac{N_{obj}(TP)}{N_{obj}(Ref)}$
Probabilistic similarity index	$\frac{2 \times \sum P_{x,gs=1}}{\sum 1_{x,gs=1} + \sum P_x}$
Probabilistic extra fraction	$\frac{\sum P_{x,gs=0}}{\sum 1_{x,gs=1}}$
Probabilistic overlap fraction	$\frac{\sum P_{x,gs=1}}{\sum 1_{x,gs=1}}$
Volume difference	$\frac{FN-FP}{2TP+FP+FN}$
Jaccard Index	$\frac{TP}{TP+FP+FN}$
Relative area error	$\frac{AS-MS}{MS}$
Hausdorf distances	$max(h(A, B), h(B, A))$ $h(A, B) = max_{a \in A} min_{b \in B} \ a - b\ $
Average distances	$max(d(A, B), d(B, A))$ $d(A, B) = \frac{1}{N} \sum_{a \in A} min_{b \in B} \ a - b\ $

method are insufficient to determine clinical applicability. For example, computational efficiency is also important in practice; and deep learning models are constrained by their computational complexity (time, memory, and power). However, with the implementation of GPU resources for training and inference, the time cost associated with deep learning methods can be significantly reduced, at the expense of an increased carbon footprint and power consumption.

VI. CONCLUSION AND FUTURE DIRECTIONS

We reviewed recent methodologies for MS lesion segmentation, with a special focus on deep-learning approaches. Statistical data from public challenges from MICCAI 2016 and ISBI 2015 facilitated comparison and evaluation of some of the most relevant methods. Despite substantial progress, there is no specific segmentation method that matches the standard of human experts. For example, in the MICCAI 2016 database,

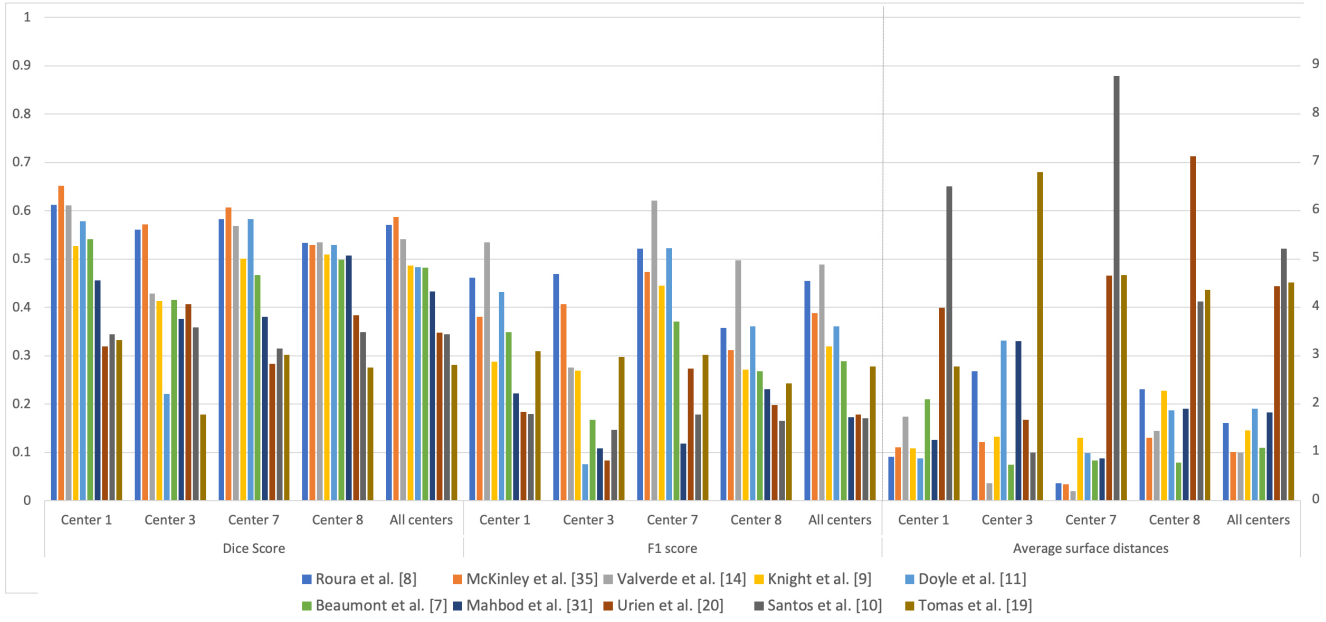


Fig. 3. Dice scores, F1 scores, and average surface distances with respect to the consensus per work participated in MICCAI 2016 for each center (and average of all centers).

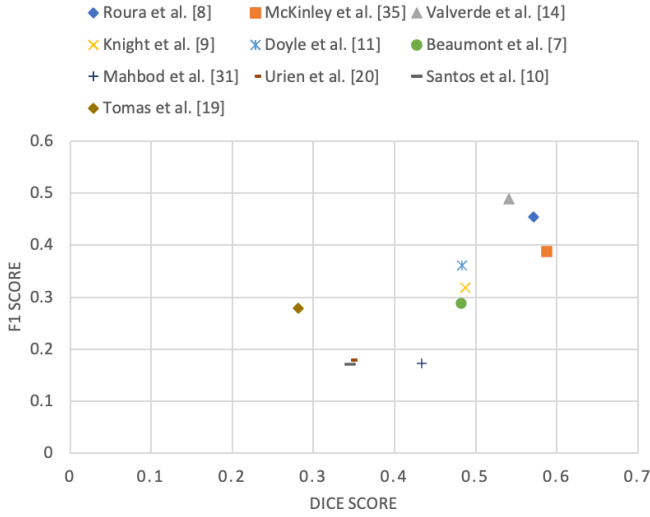


Fig. 4. Graphical results for Dice v.s. F1 score for each method from the MICCAI 2016 challenge.

the Dice score between expert raters was 0.782, while the best method [73] obtained a Dice score of 0.591 [46]. Furthermore, additional challenges, and possible future directions, for MS lesion analysis include:

A. Multi-center Studies

Private MRI databases are commonly used for designing state-of-the-art methods, some of which are not released to the research community. Conversely, publically available datasets contain a relatively small number of cases that do not represent the spectrum of real-world clinical imaging variances.

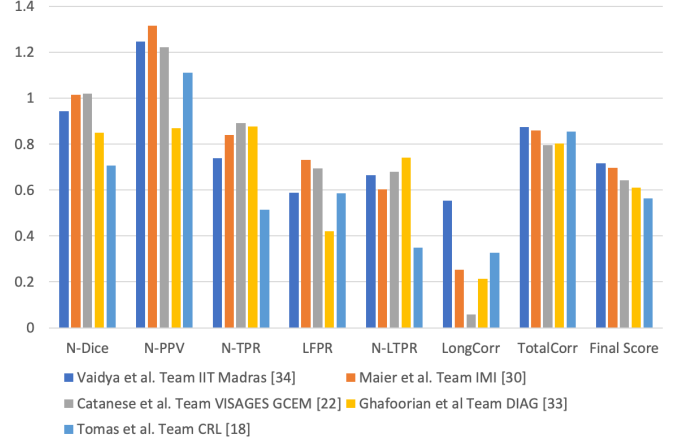


Fig. 5. Performance of the methods from ISBI 2015 evaluated with the metrics requested by the challenge. Prefix "N-" denotes that the metrics have been normalized relative to the inter-rater metrics.

Curation and sharing a sufficient amount of brain MRI data to design and analyze automatic methods is hampered by both patient privacy concerns and local governance restrictions. Separately, variances in MRI scanners (field strength, vendor, model, software) and acquisition protocols generate a wide variation in the MRI characteristics of individual subjects in any dataset. Techniques that adapt data from different sources and transfer that knowledge without additional training or labeling are therefore essential. Large multi-center studies, which capture 'real-world' variability, provide an opportunity to validate such techniques.

Perhaps the greatest challenge for deep learning applications in medical imaging is a lack of expertly annotated

data. Training a deep network for a visual task normally requires a large amount of training data to obtain the optimal outcome, and medical imaging annotation usually requires either a highly trained medical imaging analyst or an expert specialist physician/radiologist. The majority of state-of-the-art work in the field is therefore focused on either unsupervised segmentation or semi-supervised fine-tuning with domain adaptation strategies. Two new and interesting directions that could ameliorate a lack of high-quality manual annotations are weak supervision, where coarse labels (for example, image-level labels such as the number of lesions rather than their segmentation) are provided; and the use of low quality or noisy labels (for example, labels acquired at a lower resolution) [78]. Together, these strategies potentially counter the lack of dense expert annotations to deliver accurate and robust lesion segmentations.

B. Lesion Subtyping

Future segmentation strategies with multi-modal MRI input data should focus on distinguishing between multiple sclerosis lesion subtypes (such as destructive black holes, actively demyelinating, remyelinating and slowly enlarging lesions); and their functional anatomic locations. Although total lesion volume and lesion activity (the number of new and enlarging lesions measured between timepoints) constitute the most frequently employed lesion biomarkers in clinical trials, automated lesion phenotyping will potentially improve understanding of MS and its progression in individual patients by categorizing the disease into different forms and patterns. In clinical practice, patients with a substantial total lesion load may have few or even no neurological symptoms, while others with only a small number/volume of lesions may have a severe disability. This so-called “clinico-radiological paradox” is reflected in weak correlations between clinical endpoints such as the Expanded Disability Status Scale (EDSS) score and total T2 lesion load in MS clinical trials [79]. Detailed MS lesion sub-typing could potentially delineate evidence of both damage or repair within lesions, overcome the clinic-radiological paradox, and provide specific structure-function impairment information that can be exploited for individualized disease progression monitoring.

Finally, as mentioned in Section II-B, contrast-enhancing lesions, which suggest active inflammation and breakdown of the blood-brain barrier, are currently detected using gadolinium-enhanced T1 images. However, some gadolinium compounds may accumulate in the brain with repeated exposure. The detection of active inflammatory lesions without the need for contrast agents is therefore a challenging but worthwhile task suited to deep-learning techniques with multi-modal MRI training datasets.

REFERENCES

- [1] A. J. Coles, D. Compston, K. W. Selmaj, S. L. Lake, S. Moran, D. H. Margolin, K. Norris, and P. Tandon, “Alemtuzumab vs. interferon beta-1a in early multiple sclerosis,” *N Engl J Med*, vol. 359, no. 17, pp. 1786–1801, 2008.
- [2] J. H. Noseworthy, C. Lucchinetti, M. Rodriguez, and B. G. Weinshenker, “Multiple sclerosis,” *N Engl J Med*, vol. 343, no. 13, pp. 938–952, 2000.
- [3] W. H. Organization et al., “Multiple sclerosis international federation,” *Atlas: multiple sclerosis resources in the world*, 2008.
- [4] C. H. Polman, S. C. Reingold, B. Banwell, M. Clanet, J. A. Cohen, M. Filippi, K. Fujihara, E. Havrdova, M. Hutchinson, L. Kappos et al., “Diagnostic criteria for multiple sclerosis: 2010 revisions to the mcdonald criteria,” *Annals of neurology*, vol. 69, no. 2, pp. 292–302, 2011.
- [5] D. Mortazavi, A. Z. Kouzani, and H. Soltanian-Zadeh, “Segmentation of multiple sclerosis lesions in MR images: a review,” *Neuroradiology*, vol. 54, no. 4, pp. 299–320, 2012.
- [6] X. Lladó, A. Oliver, M. Cabezas, J. Freixenet, J. C. Vilanova, A. Quiles, L. Valls, L. Ramió-Torrentà, and À. Rovira, “Segmentation of multiple sclerosis lesions in brain MRI: a review of automated approaches,” *Information Sciences*, vol. 186, no. 1, pp. 164–185, 2012.
- [7] X. Lladó, O. Ganiler, A. Oliver, R. Martí, J. Freixenet, L. Valls, J. C. Vilanova, L. Ramió-Torrentà, and À. Rovira, “Automated detection of multiple sclerosis lesions in serial brain MRI,” *Neuroradiology*, vol. 54, no. 8, pp. 787–807, 2012.
- [8] D. García-Lorenzo, S. Francis, S. Narayanan, D. L. Arnold, and D. L. Collins, “Review of automatic segmentation methods of multiple sclerosis white matter lesions on conventional magnetic resonance imaging,” *Medical image analysis*, vol. 17, no. 1, pp. 1–18, 2013.
- [9] A. Danelakis, T. Theoharis, and D. A. Verganelakis, “Survey of automated multiple sclerosis lesion segmentation techniques on magnetic resonance imaging,” *Computerized Medical Imaging and Graphics*, vol. 70, pp. 83–100, 2018.
- [10] A. Kaur, L. Kaur, and A. Singh, “State-of-the-art segmentation techniques and future directions for multiple sclerosis brain lesions,” *Archives of Computational Methods in Engineering*, pp. 1–27, 2020.
- [11] H. Zhang and I. Oguz, “Multiple sclerosis lesion segmentation—a survey of supervised cnn-based methods,” *arXiv preprint arXiv:2012.08317*, 2020.
- [12] R. H. Hashemi, W. G. Bradley, and C. J. Lisanti, *MRI: the basics: The Basics*. Lippincott Williams & Wilkins, 2012.
- [13] R. E. Gabr, X. Sun, A. S. Pednekar, and P. A. Narayana, “Automated patient-specific optimization of three-dimensional double-inversion recovery magnetic resonance imaging,” *Magnetic resonance in medicine*, vol. 75, no. 2, pp. 585–593, 2016.
- [14] F. La Rosa, A. Abdulkadir, M. J. Fartaria, R. Rahmanzadeh, P.-J. Lu, R. Galbusera, M. Barakovic, J.-P. Thiran, C. Granzeria, and M. B. Cuadra, “Multiple sclerosis cortical and wm lesion segmentation at 3T MRI: a deep learning method based on FLAIR and MP2RAGE,” *NeuroImage: Clinical*, vol. 27, p. 102335, 2020.
- [15] E. Roura, M. Cabezas, S. Valverde, S. González-Villa, J. Salvi, A. Oliver, and X. Lladó, “Unsupervised multiple sclerosis lesion detection and segmentation using rules and level sets,” *MSSEG Challenge Proceedings: Multiple Sclerosis Lesions Segmentation Challenge Using a Data Management and Processing Infrastructure*, p. 51, 2016.
- [16] M. M. Santos, P. Diniz, A. G. Silva-Filho, and W. P. Santos, “Evaluation-oriented training strategy on MS segmentation challenge 2016,” *Proceedings of the 1st MICCAI Challenge on Multiple Sclerosis Lesions Segmentation Challenge Using a Data Management and Processing Infrastructure-MICCAI-MSSEG*, pp. 57–62, 2016.
- [17] J. Beaumont, O. Commowick, and C. Barillot, “Automatic multiple sclerosis lesion segmentation from intensity-normalized multi-channel MRI,” in *Proceedings of the 1st MICCAI Challenge on Multiple Sclerosis Lesions Segmentation Challenge Using a Data Management and Processing Infrastructure - MICCAI-MSSEG*. Springer, 2016.
- [18] S. Valverde, M. Cabezas, E. Roura, S. González-Villa, J. Salvi, A. Oliver, and X. Lladó, “Multiple sclerosis lesion detection and segmentation using a convolutional neural network of 3D patches,” *MSSEG Challenge Proceedings: Multiple Sclerosis Lesions Segmentation Challenge Using a Data Management and Processing Infrastructure*, p. 75, 2016.
- [19] E. Bardin, S. Ourselin, D. Dormont, G. Malandain, D. Tancé, K. Parain, N. Ayache, and J. Yelnik, “Co-registration of histological, optical and MR data of the human brain,” in *International conference on medical image computing and computer-assisted intervention*. Springer, 2002, pp. 548–555.
- [20] S. J. Kiebel, J. Ashburner, J.-B. Poline, and K. J. Friston, “MRI and PET coregistration—a cross validation of statistical parametric mapping and automated image registration,” *Neuroimage*, vol. 5, no. 4, pp. 271–279, 1997.

- [21] J. Knight and A. Khademi, "MS lesion segmentation using FLAIR MRI only," *Proceedings of the 1st MICCAI Challenge on Multiple Sclerosis Lesions Segmentation Challenge Using a Data Management and Processing Infrastructure-MICCAI-MSSEG*, pp. 21–28, 2016.
- [22] S. Doyle, F. Forbes, and M. Dojat, "Automatic multiple sclerosis lesion segmentation with p-locus," in *Proceedings of the 1st MICCAI Challenge on Multiple Sclerosis Lesions Segmentation Challenge Using a Data Management and Processing Infrastructure - MICCAI-MSSEG*. Springer, 2016, pp. 17–21.
- [23] A. Jog, A. Carass, D. L. Pham, and J. L. Prince, "Multi-output decision trees for lesion segmentation in multiple sclerosis," in *Medical Imaging 2015: Image Processing*, vol. 9413. International Society for Optics and Photonics, 2015, p. 94131C.
- [24] S. Roy, J. A. Butman, D. S. Reich, P. A. Calabresi, and D. L. Pham, "Multiple sclerosis lesion segmentation from brain MRI via fully convolutional neural networks," *arXiv preprint arXiv:1803.09172*, 2018.
- [25] J. E. Iglesias, C.-Y. Liu, P. M. Thompson, and Z. Tu, "Robust brain extraction across datasets and comparison with publicly available methods," *IEEE Transactions on Medical Imaging*, vol. 30, no. 9, pp. 1617–1634, 2011.
- [26] N. Weiss, D. Rueckert, and A. Rao, "Multiple sclerosis lesion segmentation using dictionary learning and sparse coding," in *International Conference on Medical Image Computing and Computer-Assisted Intervention*. Springer, 2013, pp. 735–742.
- [27] S. Roy, D. Bhattacharyya, S. K. Bandyopadhyay, and T.-H. Kim, "An effective method for computerized prediction and segmentation of multiple sclerosis lesions in brain MRI," *Computer methods and programs in biomedicine*, vol. 140, pp. 307–320, 2017.
- [28] J. Hill, K. Matlock, B. Nutter, and S. Mitra, "Automated segmentation of MS lesions in MR images based on an information theoretic clustering and contrast transformations," *Technologies*, vol. 3, no. 2, pp. 142–161, 2015.
- [29] X. Tomas-Fernandez and S. K. Warfield, "A model of population and subject (mops) intensities with application to multiple sclerosis lesion segmentation," *IEEE transactions on medical imaging*, vol. 34, no. 6, pp. 1349–1361, 2015.
- [30] —, "MRI robust brain tissue segmentation with application to multiple sclerosis," *Proceedings of the 1st MICCAI Challenge on Multiple Sclerosis Lesions Segmentation Challenge Using a Data Management and Processing Infrastructure-MICCAI-MSSEG*, pp. 63–67, 2016.
- [31] H. Urien, I. Buvat, N. Rougon, and I. Bloch, "A 3D hierarchical multimodal detection and segmentation method for multiple sclerosis lesions in MRI," in *Proceedings of the 1st MICCAI Challenge on Multiple Sclerosis Lesions Segmentation Challenge Using a Data Management and Processing Infrastructure - MICCAI-MSSEG*. Springer, 2016, pp. 69–74.
- [32] S. Koley, C. Chakraborty, C. Mainero, B. Fischl, and I. Aganj, "A fast approach to automatic detection of brain lesions," in *International Workshop on Brainlesion: Glioma, Multiple Sclerosis, Stroke and Traumatic Brain Injuries*. Springer, 2016, pp. 52–61.
- [33] L. Catanese, O. Commowick, and C. Barillot, "Automatic graph cut segmentation of multiple sclerosis lesions," in *ISBI Longitudinal Multiple Sclerosis Lesion Segmentation Challenge*. IEEE, 2015.
- [34] J. Beaumont, O. Commowick, and C. Barillot, "Multiple sclerosis lesion segmentation using an automated multimodal graph cut," in *Proceedings of the 1st MICCAI Challenge on Multiple Sclerosis Lesions Segmentation Challenge Using a Data Management and Processing Infrastructure - MICCAI-MSSEG*. Springer, 2016, pp. 1–8.
- [35] S. Andermatt, S. Pezold, and P. C. Cattin, "Automated segmentation of multiple sclerosis lesions using multi-dimensional gated recurrent units," in *International MICCAI Brainlesion Workshop*. Springer, 2017, pp. 31–42.
- [36] M. Havaei, N. Guizard, N. Chapados, and Y. Bengio, "Hemis: Heteromodal image segmentation," in *International Conference on Medical Image Computing and Computer-Assisted Intervention*. Springer, 2016, pp. 469–477.
- [37] C. Zhang, Y. Song, S. Liu, S. Lill, C. Wang, Z. Tang, Y. You, Y. Gao, A. Klitorner, M. Barnett *et al.*, "MS-GAN: GAN-based semantic segmentation of multiple sclerosis lesions in brain magnetic resonance imaging," in *2018 Digital Image Computing: Techniques and Applications (DICTA)*. IEEE, 2018, pp. 1–8.
- [38] A. Ackaouy, N. Courty, E. Vallee, O. Commowick, C. Barillot, and F. Galassi, "Unsupervised domain adaptation with optimal transport in multi-site segmentation of multiple sclerosis lesions from MRI data," *Frontiers in Computational Neuroscience*, vol. 14, 2020.
- [39] M. D. Steenwijk, P. J. Pouwels, M. Daams, J. W. van Dalen, M. W. Caan, E. Richard, F. Barkhof, and H. Vrenken, "Accurate white matter lesion segmentation by k nearest neighbor classification with tissue type priors (knn-tps)," *NeuroImage: Clinical*, vol. 3, pp. 462–469, 2013.
- [40] E. Geremia, B. H. Menze, and N. Ayache, "Spatially adaptive random forests," in *2013 IEEE 10th International Symposium on Biomedical Imaging*. IEEE, 2013, pp. 1344–1347.
- [41] O. Maier and H. Handels, "MS lesion segmentation in MRI with random forests," *Proc. 2015 Longitudinal Multiple Sclerosis Lesion Segmentation Challenge*, pp. 1–2, 2015.
- [42] A. Mahbod, C. Wang, and O. Smedby, "Automatic multiple sclerosis lesion segmentation using hybrid artificial neural networks," *MSSEG Challenge Proceedings: Multiple Sclerosis Lesions Segmentation Challenge Using a Data Management and Processing Infrastructure*, vol. 29, 2016.
- [43] A. Doyle, C. Elliott, Z. Karimaghloo, N. Subbanna, D. L. Arnold, and T. Arbel, "Lesion detection, segmentation and prediction in multiple sclerosis clinical trials," in *International MICCAI Brainlesion Workshop*. Springer, 2017, pp. 15–28.
- [44] M. Ghafoorian and B. Platel, "Convolutional neural networks for MS lesion segmentation, method description of diag team," *Proceedings of the 2015 Longitudinal Multiple Sclerosis Lesion Segmentation Challenge*, pp. 1–2, 2015.
- [45] S. Vaidya, A. Chunduru, R. Muthuganapathy, and G. Krishnamurthi, "Longitudinal multiple sclerosis lesion segmentation using 3D convolutional neural networks," *Proceedings of the 2015 Longitudinal Multiple Sclerosis Lesion Segmentation Challenge*, pp. 1–2, 2015.
- [46] R. McKinley, R. Wepfer, T. Gundersen, F. Wagner, A. Chan, R. Wiest, and M. Reyes, "Nabla-net: A deep dag-like convolutional architecture for biomedical image segmentation," in *International Workshop on Brainlesion: Glioma, Multiple Sclerosis, Stroke and Traumatic Brain Injuries*. Springer, 2016, pp. 119–128.
- [47] T. Brosch, L. Y. Tang, Y. Yoo, D. K. Li, A. Traboulsee, and R. Tam, "Deep 3D convolutional encoder networks with shortcuts for multiscale feature integration applied to multiple sclerosis lesion segmentation," *IEEE transactions on medical imaging*, vol. 35, no. 5, pp. 1229–1239, 2016.
- [48] S. Valverde, M. Cabezas, E. Roura, S. González-Villà, D. Pareto, J. C. Vilanova, L. Ramió-Torrentà, À. Rovira, A. Oliver, and X. Lladó, "Improving automated multiple sclerosis lesion segmentation with a cascaded 3D convolutional neural network approach," *NeuroImage*, vol. 155, pp. 159–168, 2017.
- [49] F. Isensee, J. Petersen, A. Klein, D. Zimmerer, P. F. Jaeger, S. Kohl, J. Wasserthal, G. Koehler, T. Norajitra, S. Wirkert *et al.*, "nnu-net: Self-adapting framework for u-net-based medical image segmentation," *arXiv preprint arXiv:1809.10486*, 2018.
- [50] T. Nair, D. Precup, D. L. Arnold, and T. Arbel, "Exploring uncertainty measures in deep networks for multiple sclerosis lesion detection and segmentation," *Medical image analysis*, vol. 59, p. 101557, 2020.
- [51] O. Ronneberger, P. Fischer, and T. Brox, "U-net: Convolutional networks for biomedical image segmentation," in *International Conference on Medical image computing and computer-assisted intervention*. Springer, 2015, pp. 234–241.
- [52] Ö. Çiçek, A. Abdulkadir, S. S. Lienkamp, T. Brox, and O. Ronneberger, "3D U-Net: learning dense volumetric segmentation from sparse annotation," in *International conference on medical image computing and computer-assisted intervention*. Springer, 2016, pp. 424–432.
- [53] R. McKinley, R. Wepfer, L. Grunder, F. Aschwanden, T. Fischer, C. Friedli, R. Muri, C. Rummel, R. Verma, C. Weisstanner *et al.*, "Automatic detection of lesion load change in multiple sclerosis using convolutional neural networks with segmentation confidence," *NeuroImage: Clinical*, vol. 25, p. 102104, 2020.
- [54] R. McKinley, R. Wepfer, F. Aschwanden, L. Grunder, R. Muri, C. Rummel, R. Verma, C. Weisstanner, M. Reyes, A. Salmen *et al.*, "Simultaneous lesion and brain segmentation in multiple sclerosis using deep neural networks," *Scientific Reports*, 2021.
- [55] Y. Gal and Z. Ghahramani, "Dropout as a bayesian approximation: Representing model uncertainty in deep learning," in *international conference on machine learning*, 2016, pp. 1050–1059.
- [56] J. Chung, C. Gulcehre, K. Cho, and Y. Bengio, "Empirical evaluation of gated recurrent neural networks on sequence modeling," *NeurIPS 2014 Deep Learning and Representation Learning Workshop*, 2014.

- [57] F. Isensee, P. F. Jaeger, S. A. A. Kohl, and K. H. Maier-Hein, “nnU-Net: a self-configuring method for deep learning-based biomedical image segmentation,” *Nature: Methods*, 2021.
- [58] O. Ganiler, A. Oliver, Y. Díez, J. Freixenet, J. C. Vilanova, B. Beltran, L. Ramió-Torrentà, À. Rovira, and X. Lladó, “A subtraction pipeline for automatic detection of new appearing multiple sclerosis lesions in longitudinal studies,” *Neuroradiology*, vol. 56, no. 5, pp. 363–374, 2014.
- [59] M. Cabezas, J. Corral, A. Oliver, Y. Díez, M. Tintoré, C. Auger, X. Montalbán, X. Lladó, D. Pareto, and À. Rovira, “Improved automatic detection of new T2 lesions in multiple sclerosis using deformation fields,” *American Journal of Neuroradiology*, vol. 37, no. 10, pp. 1816–1823, 2016.
- [60] S. Jain, A. Ribbens, D. M. Sima, M. Cambron, J. De Keyser, C. Wang, M. H. Barnett, S. Van Huffel, F. Maes, and D. Smeets, “Two time point MS lesion segmentation in brain MRI: an expectation-maximization framework,” *Frontiers in neuroscience*, vol. 10, p. 576, 2016.
- [61] S. Jain, D. M. Sima, A. Ribbens, M. Cambron, A. Maertens, W. Van Hecke, J. De Mey, F. Barkhof, M. D. Steenwijk, M. Daams *et al.*, “Automatic segmentation and volumetry of multiple sclerosis brain lesions from MR images,” *NeuroImage: Clinical*, vol. 8, pp. 367–375, 2015.
- [62] P. Schmidt, V. Pongratz, P. Kuster, D. Meier, J. Wuerfel, C. Lukas, B. Bellenberg, F. Zipp, S. Groppa, P. G. Samann, F. Webber, C. Gaser, T. Franke, M. Bussas, J. Kirschke, C. Zimmer, B. Hemmer, and M. Muhlau, “Automated segmentation of changes in FLAIR-hyperintense white matter lesions in multiple sclerosis on serial magnetic resonance imaging,” *Neuroimage: Clinical*, 2019.
- [63] P. Schmidt, C. Gaser, M. Arsic, D. Buck, A. Forschler, A. Berthele, M. Hoshi, R. Ilg, V. J. Schmid, C. Zimmer, B. Hemmer, and M. Muhlau, “Aan automated tool for detection of FLAIR-hyperintense white-matter lesions in Multiple Sclerosis,” *Neuroimage*, 2012.
- [64] S. Cerri, A. Hoopes, D. N. Greve, M. Muhlau, and K. Van Leemput, “A longitudinal method for simultaneous whole-brain and lesion segmentation in multiple sclerosis,” *arXiv preprint arXiv:2008.05117*, 2020.
- [65] S. Cerri, O. Puonti, D. S. Meier, J. Wuerfel, M. Muhlau, H. R. Siebner, and K. Van Leemput, “A contrast-adaptive method for simultaneous whole-brain and lesion segmentation in multiple sclerosis,” *arXiv preprint arXiv:2005.05135*, 2020.
- [66] M. Salem, S. Valverde, M. Cabezas, D. Pareto, A. Oliver, J. Salvi, À. Rovira, and X. Lladó, “A fully convolutional neural network for new t2-w lesion detection in multiple sclerosis,” *NeuroImage: Clinical*, vol. 25, p. 102149, 2020.
- [67] N. Gessert, J. Krüger, R. Opfer, A.-C. Ostwaldt, P. Manogaran, H. H. Kitzler, S. Schippling, and A. Schlaefer, “Multiple sclerosis lesion activity segmentation with attention-guided two-path cnns,” *Computerized Medical Imaging and Graphics*, p. 101772, 2020.
- [68] A. Vaswani, N. Shazeer, N. Parmar, J. Uszkoreit, L. Jones, A. N. Gomez, Ł. Kaiser, and I. Polosukhin, “Attention is all you need,” in *Advances in neural information processing systems*, 2017, pp. 5998–6008.
- [69] N. Gessert, M. Bengs, J. Krüger, R. Opfer, A.-C. Ostwaldt, P. Manogaran, S. Schippling, and A. Schlaefer, “4D deep learning for multiple sclerosis lesion activity segmentation,” *arXiv preprint arXiv:2004.09216*, 2020.
- [70] M. Ghafoorian, A. Mehrtaash, T. Kapur, N. Karssemeijer, E. Marchiori, M. Pesteie, C. R. Guttmann, F.-E. de Leeuw, C. M. Tempny, B. Van Ginneken *et al.*, “Transfer learning for domain adaptation in MRI: Application in brain lesion segmentation,” in *International conference on medical image computing and computer-assisted intervention*. Springer, 2017, pp. 516–524.
- [71] S. Valverde, M. Salem, M. Cabezas, D. Pareto, J. C. Vilanova, L. Ramió-Torrentà, À. Rovira, J. Salvi, A. Oliver, and X. Lladó, “One-shot domain adaptation in multiple sclerosis lesion segmentation using convolutional neural networks,” *NeuroImage: Clinical*, vol. 21, p. 101638, 2019.
- [72] K. Kamnitsas, C. Baumgartner, C. Ledig, V. Newcombe, J. Simpson, A. Kane, D. Menon, A. Nori, A. Criminisi, D. Rueckert *et al.*, “Unsupervised domain adaptation in brain lesion segmentation with adversarial networks,” in *International conference on information processing in medical imaging*. Springer, 2017, pp. 597–609.
- [73] J. A. Palladino, D. F. Slezak, and E. Ferrante, “Unsupervised domain adaptation via cyclegan for white matter hyperintensity segmentation in multicenter MR images,” *arXiv preprint arXiv:2009.04985*, 2020.
- [74] J.-Y. Zhu, T. Park, P. Isola, and A. A. Efros, “Unpaired image-to-image translation using cycle-consistent adversarial networks,” in *Proceedings of the IEEE international conference on computer vision*, 2017, pp. 2223–2232.
- [75] B. E. Dewey, C. Zhao, J. C. Reinhold, A. Carass, K. C. Fitzgerald, E. S. Sotirchos, S. Saidha, J. Oh, D. L. Pham, P. A. Calabresi *et al.*, “DeepHarmony: a deep learning approach to contrast harmonization across scanner changes,” *Magnetic resonance imaging*, vol. 64, pp. 160–170, 2019.
- [76] A. Carass, S. Roy, A. Jog, J. L. Cuzzocreo, E. Magrath, A. Gherman, J. Button, J. Nguyen, F. Prados, C. H. Sudre *et al.*, “Longitudinal multiple sclerosis lesion segmentation: resource and challenge,” *NeuroImage*, vol. 148, pp. 77–102, 2017.
- [77] O. Commowick, A. Istace, M. Kain, B. Laurent, F. Leray, M. Simon, S. C. Pop, P. Girard, R. Ameli, J.-C. Ferré *et al.*, “Objective evaluation of multiple sclerosis lesion segmentation using a data management and processing infrastructure,” *Scientific reports*, vol. 8, no. 1, pp. 1–17, 2018.
- [78] G. Papandreou, L.-C. Chen, K. P. Murphy, and A. L. Yuille, “Weakly-and semi-supervised learning of a deep convolutional network for semantic image segmentation,” in *Proceedings of the IEEE international conference on computer vision*, 2015, pp. 1742–1750.
- [79] K. Hackmack, M. Weygandt, J. Wuerfel, C. F. Pfueller, J. Bellmann-Strobl, F. Paul, and J.-D. Haynes, “Can we overcome the ‘clinico-radiological paradox’ in multiple sclerosis?” *Journal of neurology*, vol. 259, no. 10, pp. 2151–2160, 2012.